

Effect mechanism of aluminum occurrence and content on the induration characteristics of iron ore pellets

Hongyu Tian, Deqing Zhu, Jian Pan, Congcong Yang, Weiqun Huang, and Mansheng Chu

Cite this article as:

Hongyu Tian, Deqing Zhu, Jian Pan, Congcong Yang, Weiqun Huang, and Mansheng Chu, Effect mechanism of aluminum occurrence and content on the induration characteristics of iron ore pellets, *Int. J. Miner. Metall. Mater.*, 30(2023), No. 12, pp. 2334-2346. <https://doi.org/10.1007/s12613-023-2725-3>

View the article online at [SpringerLink](#) or [IJMMM Webpage](#).

Articles you may be interested in

Anand Babu Kotta, Anshuman Patra, Mithilesh Kumar, and Swapan Kumar Karak, [Effect of molasses binder on the physical and mechanical properties of iron ore pellets](#), *Int. J. Miner. Metall. Mater.*, 26(2019), No. 1, pp. 41-51. <https://doi.org/10.1007/s12613-019-1708-x>

Cui Wang, Chen-yang Xu, Zheng-jian Liu, Yao-zu Wang, Rong-rong Wang, and Li-ming Ma, [Effect of organic binders on the activation and properties of indurated magnetite pellets](#), *Int. J. Miner. Metall. Mater.*, 28(2021), No. 7, pp. 1145-1152. <https://doi.org/10.1007/s12613-020-2055-7>

Wen-tao Zhou, Yue-xin Han, Yong-sheng Sun, and Yan-jun Li, [Strengthening iron enrichment and dephosphorization of high-phosphorus oolitic hematite using high-temperature pretreatment](#), *Int. J. Miner. Metall. Mater.*, 27(2020), No. 4, pp. 443-453. <https://doi.org/10.1007/s12613-019-1897-3>

Li-xin Qian, Tie-jun Chun, Hong-ming Long, and Qing-min Meng, [Detection of the assimilation characteristics of iron ores: Dynamic resistance measurements](#), *Int. J. Miner. Metall. Mater.*, 27(2020), No. 1, pp. 18-25. <https://doi.org/10.1007/s12613-019-1869-7>

Shi-chao Wu, Zheng-yao Li, Ti-chang Sun, Jue Kou, and Xiao-hui Li, [Effect of additives on iron recovery and dephosphorization by reduction roasting–magnetic separation of refractory high-phosphorus iron ore](#), *Int. J. Miner. Metall. Mater.*, 28(2021), No. 12, pp. 1908-1916. <https://doi.org/10.1007/s12613-021-2329-8>

Wei Li, Nan Wang, Gui-qin Fu, Man-sheng Chu, and Miao-yong Zhu, [Effect of Cr₂O₃ addition on the oxidation induration mechanism of Hongge vanadium titanomagnetite pellets](#), *Int. J. Miner. Metall. Mater.*, 25(2018), No. 4, pp. 391-398. <https://doi.org/10.1007/s12613-018-1583-x>




IJMMM WeChat



QQ author group

Effect mechanism of aluminum occurrence and content on the induration characteristics of iron ore pellets

Hongyu Tian¹, Deqing Zhu², Jian Pan², Congcong Yang²,, Weiqun Huang³, and Mansheng Chu^{1,4}

1) School of Metallurgy, Northeastern University, Shenyang 110819, China

2) School of Minerals Processing and Bioengineering, Central South University, Changsha 410083, China

3) Ecological Geology Brigade of Jiangxi Geological Bureau, Nanchang 330030, China

4) Engineering Research Center of Frontier Technologies for Low-carbon Steelmaking (Ministry of Education), Shenyang 110819, China

(Received: 31 March 2023; revised: 20 July 2023; accepted: 11 August 2023)

Abstract: With the intensified depletion of high-grade iron ores, the increased aluminum content in iron ore concentrates has become unavoidable, which is detrimental to the pelletization process. Therefore, the effect mechanism of aluminum on pellet quality must be identified. In this study, the influence of aluminum occurrence and content on the induration of hematite (H) and magnetite (M) pellets was investigated through the addition of corresponding Al-containing additives, including alumina, alumogothite, gibbsite, and kaolinite. Systematic mineralogical analysis, combined with the thermodynamic properties of different aluminum occurrences and the quantitative characterization of consolidation behaviors, were conducted to determine the related mechanism. The results showed that the alumina from various aluminum occurrences adversely affected the induration characteristics of pellets, especially at an aluminum content of more than 2.0wt%. The thermal decomposition of gibbsite and kaolinite tends to generate internal stress and fine cracks, which hinder the respective microcrystalline bonding and recrystallization between Fe₂O₃ particles. The adverse effect on the induration characteristics of fired pellets with different aluminum occurrences can be relieved to varying degrees through the formation of liquid phase bonds between the hematite particles. Kaolinite is more beneficial to the induration process than the other three aluminum occurrences because of the formation of more liquid phase, which improves pellet consolidation. The research results can further provide insights into the effect of aluminum occurrence and content in iron ore concentrates on downstream processing and serve as a guide for the utilization of high-alumina iron ore concentrates in pelletization.


Keywords: iron ore; pellet; aluminum occurrence; consolidation behavior; element migration

1. Introduction

Oxidized pellets are characterized by high iron grade, desirable cold compressive strength (CCS), preferable metallurgical performance, low environmental pollution, and energy-saving production, and they have become one of the important burdens in modern blast furnaces [1–3]. Given the severe shortage of high-quality pellet feeds in China, the high external dependence of the country on overseas iron ores has become unavoidable [4–5]. However, the constant consumption and gradual scarcity of high-quality iron ore resources have resulted in an evident increase in the usage proportion of off-grade iron ores with relatively large quantities of impurities (Al₂O₃, SiO₂, P, S, etc.) [6–7]. Therein, the utilization of high-alumina iron ores has become a concerning problem in the production process of oxidized pellets and the subsequent blast furnace processing. The Al₂O₃ content of pellets is suggested to be less than 0.9wt% [8]. However, the Al₂O₃ in iron ore concentrates from the main importing countries, i.e., Australia and Brazil, can reach 2.16wt% and 1.54wt%, respectively [9]. Domestic iron ore concentrates

contain up to 1.5wt% Al₂O₃ content after mineral processing [10].

Previous studies have proved the huge effect of Al₂O₃ content in pellets on the properties of oxidized pellets. When the Al₂O₃ content was increased from natural content (0.75wt%) to 1.5wt% in magnetite pellets via the addition of Al₂O₃ analytic reagent as an aluminum source, the CCS of fired pellets climbed from 3307 up to 3403 N per pellet. However, the CCS declined to 2855 N per pellet when the Al₂O₃ content was increased continuously to 2.5wt% [11]; this finding implies the two-sided effect of aluminum on the quality of oxidized pellets. On the one hand, a small quantity of Al₂O₃ can help form 2FeO·2Al₂O₃·5SiO₂ by replacing the FeO and Fe₃O₄ from the fayalite phases (e.g., 2FeO·SiO₂–FeO and 2FeO·SiO₂–Fe₃O₄) at 1083°C. The free FeO and Fe₃O₄ can increase the recrystallization and grain growth of Fe₂O₃ and improve the consolidation efficiency of pellets [12–14]. On the other hand, an excess Al₂O₃ content impedes mass transfer among crystal lattices because of its low reactivity and restricts the growth of crystalline grains, which results in the low mechanical strength of pellets

 Corresponding author: Congcong Yang E-mail: smartyoung@csu.edu.cn

© University of Science and Technology Beijing 2023

[15–16]. Furthermore, an excess Al₂O₃ content increases the melting temperature and viscosity of liquid phases, which adversely affects the improvement of liquid bonding phases [17]. The weakened consolidation of oxidized pellets results in an inferior pellet structure and low CCS of the fired pellets [18]. Furthermore, fired pellets with a low CCS exhibit an unsatisfactory metallurgical performance, especially in reduction swelling and reduction degradation [19–21].

The investigation regarding the effect of Al₂O₃ content on the properties of pellets has shown big progress in the past several years. However, in the above studies, the Al₂O₃ analytic reagent was mainly employed as an Al-containing additive. In reality, the occurrence states of aluminum in iron ores mainly include gibbsite, diaspore, kaolinite, aluminogothite, etc. [22]. Furthermore, the Al-containing minerals characterized by a complicated and fine-grained dissemination form different symbiotic relationships with iron oxides and other gangue minerals [23]. In this study, four different Al-containing additives (alumina, hercynite, gibbsite, and kaolinite) were used to investigate the effects of aluminum occurrence and content on the properties of hematite (H) and magnetite (M) pellets. The influences of the occurrence states of aluminum on the microstructure and consolidation efficiency of fired pellets were also revealed. The findings of the present study can aid in gaining further insights into the influence of aluminum in natural iron ores on downstream processing and guide the utilization of high-alumina iron ore concentrates in pelletization.

2. Experimental

2.1. Materials

2.1.1. Iron ore concentrate

Table 1 presents the chemical composition of the as-received hematite (H) and magnetite (M) concentrates, from Brazil and China, respectively, used in this study. The results indicate that H and M concentrates both have high iron grades of 66.29wt% and 68.31wt% with different Fe₃O₄ contents of 0.97wt% and 69.37wt%, respectively. Meanwhile, the contents of SiO₂ and Al₂O₃ in H concentrate are 3.90wt% and 0.30wt%, respectively, which are slightly higher than those in M concentrate. Besides, H and M concentrates have low contents of S and P. Fig. 1 illustrates the X-ray diffraction (XRD) patterns of the two types of iron ores. The figure indicates that H and M concentrates mainly consist of hematite (Fe₂O₃) and magnetite (Fe₃O₄), respectively. Both contain a fraction of quartz (SiO₂).

Table 2 shows the size distribution and specific surface area of iron ore concentrates. H and M concentrates have a fineness of 98.62% and 97.48% passing 0.074 mm and specific surface areas of 1533 and 1549 cm²·g⁻¹, respectively. Hence, both meet the pelletization requirements.

2.1.2. Al-containing additives

Four Al-containing additives, i.e., alumina (Al₂O₃), hercynite (FeO·Al₂O₃), gibbsite (Al(OH)₃), and kaolinite (Al₂O₃·2SiO₂·2H₂O), were used to reveal the effect of aluminum occurrence and content on the properties of oxidized

Table 1. Chemical composition of iron ore concentrates

Concentrate	TFe	Fe ₂ O ₃	Fe ₃ O ₄	SiO ₂	Al ₂ O ₃	CaO	MgO	S	P	LOI
H	66.29	94.07	0.97	3.90	0.30	0.11	0.02	0.005	0.021	0.53
M	68.31	29.08	69.37	3.78	0.08	0.10	0.09	0.049	0.009	-2.62

Note: TFe—total Fe element; LOI—loss on ignition.

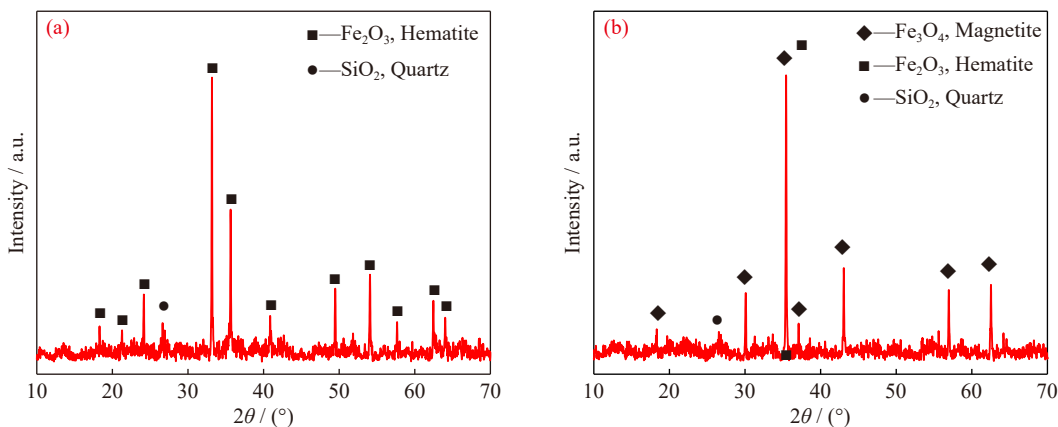


Fig. 1. XRD patterns of iron ore concentrates: (a) hematite concentrate; (b) magnetite concentrate.

Table 2. Size distribution and specific surface area of iron ore concentrates

Concentrate	Size distribution / wt%				Specific surface areas (Blaine index) / (cm ² ·g ⁻¹)
	+0.074 mm	0.043–0.074 mm	0.025–0.043 mm	–0.025	
H	1.38	3.19	17.71	77.71	1533
M	2.52	11.99	25.64	59.85	1549

pellets. The particle size of Al-containing additives was less than 0.5 mm (80% passing 0.074 mm). Therein, (1) alumina and gibbsite were analytic reagents; (2) hercynite was produced using a high-temperature sintering method applied in

industrial production to replace alumogothite; (3) kaolinite was a natural mineral that after washing and desliming pre-treatment. Table 3 and Fig. 2 show the chemical composition and XRD pattern of the Al-containing additives, respectively.

Table 3. Chemical composition of Al-containing additives

Additive	TFe	FeO	Al ₂ O ₃	SiO ₂	CaO	MgO	S	P	LOI
Alumina	—	—	99.25	0.17	0.20	—	—	—	0.38
Hercynite	31.65	26.99	50.58	0.59	0.74	1.17	0.014	0.074	-2.87
Gibbsite	—	—	64.65	0.03	0.01	—	—	—	33.37
Kaolinite	0.99	—	33.49	46.24	0.11	0.34	0.038	0.007	11.15

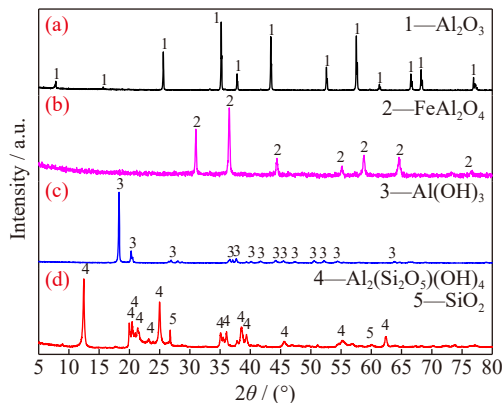


Fig. 2. XRD pattern of Al-containing additives: (a) alumina; (b) hercynite; (c) gibbsite; (d) kaolinite.

According to Table 3, alumina has a high aluminum content of 99.25wt%, and kaolinite mainly contains a low Al₂O₃ content of 33.49wt% and a high SiO₂ content of 46.24wt%, with an LOI of 11.15wt%. Hercynite is a spinel phase that mainly contains 50.58wt% Al₂O₃, 31.65wt% Fe, and

26.99wt% FeO, whereas gibbsite has a relatively high aluminum content of 64.65wt% with a high LOI of 33.37wt%. Fig. 2 displays the occurrence states of aluminum in different additives. The chemical compositions of the four Al-containing additives also showed good agreement with the major mineral phases analyzed using the XRD patterns.

2.1.3. Binder

A kind of bentonite from India was used as a binder to improve the ballability of iron ore concentrates. Table 4 provides the chemical compositions of bentonite, while Table 5 shows its size distributions and physical properties. Bentonite has a high montmorillonite content of 84.73wt% and moisture absorption of 569vol%, indicating its good performance in accordance with the Chinese standard GB/T 20973-2020.

Table 4. Chemical composition of bentonite

TFe	SiO ₂	CaO	MgO	Al ₂ O ₃	S	P	LOI
11.12	47.90	1.59	—	14.81	—	0.057	15.25

Table 5. Size distributions and physical properties of bentonite

Size distribution / wt%		COI / [%·(5 g ⁻¹)]	SV / (mL·g ⁻¹)	MA (2 h) / vol%	MBA / [g·(100 g ⁻¹)]	MC / wt%
-0.075 mm	-0.045 mm					
92.46	68.58	100	14	569	37.45	84.73

Note: COI—colloid index; SV—swelling volume; MA—moisture absorption; MBA—methylene blue adsorbed; MC—montmorillonite content.

2.1.4. Flux

To improve the roasting performance and consolidation of H pellets, analytic-grade calcium carbonate powder with 100% passing 0.074 mm was employed to adjust the binary basicity *R* (mass ratio of CaO to SiO₂) of pellets for all cases.

2.2. Methods

2.2.1. Preheating and roasting tests for oxidized pellets of iron ore concentrates

The iron ore concentrate was mixed well with a fixed proportion of 1.4wt% bentonite and a required ratio of Al-containing additives (natural content of Al₂O₃, 1.0wt%, 2.0wt%, and 3.0wt% for pellets) and suitable water. H pellet has a 0.3 binary basicity adjusted by calcium carbonate, and M pellet has a natural binary basicity (*R* = 0.03). Then, approximately 4 kg mixtures were slowly added to a disk pelletizer with a diameter of 800 mm, an incline angle of 47° to the horizon,

and a speed of 25 revolutions per minute for pelletization for a balling time of 14 min. The qualified green balls with sizes between 10 and 16 mm were sorted and then dried at 105°C for 3 h in a drying oven.

The bench-scale preheating and roasting tests of H (M) pellets were performed in an electric tube furnace under preheating at 950°C (900°C) for 15 min (i.e., preheated pellets) in combination with roasting at 1250°C (1200°C) for 15 min (i.e., fired pellets). Then, the preheated and fired pellets were cooled for subsequent measurement of CCS.

2.2.2. Characterization methodology

Chemical analysis methods were used to determine the chemical composition of raw materials. The specific surface area of iron ore concentrates was measured in the Blaine index in accordance with the Chinese standard GB/T 8074. The chemical composition, size distributions, and physical properties of bentonite were measured in accordance with the

Chinese standard GB/T 20973-2007.

With the use of a simultaneous thermal analyzer (Netzsch STA449F3), the thermogravimetry–derivative thermogravimetry–differential scanning calorimetry (TG–DTG–DSC) was carried out on the four Al-containing additives to reveal their thermodynamic properties during oxidation and induration processes at the temperature-rise period. In thermogravimetric experiments, approximately 20 mg of finely ground Al-containing additives were used at the temperature range of 25–1250°C and under an air atmosphere with a flow rate of 50 cm³/min and a heating rate of 10°C/min.

The XRD instrument (SIMENS D500) and MDI Jade 6.0 software were used to determine the phase composition of Al-containing additives. XRD tests were conducted under a Cu K_α source, a wavelength of 1.54056 Å, a scanning angle range of 2θ = 5°–80°, and a step size of 0.02°.

To demonstrate the effect of aluminum occurrence and content on the induration characteristics of H and M pellets, the microstructure of preheated and fired pellets was further identified by applying scanning electron microscopy (SEM, MIRA3 LMH, TESCAN Ltd., Czech Republic) and energy disperse spectroscopy (EDS, Oxford X MAX20, England). SEM images were recorded in backscatter electron modes operating at a low vacuum of 0.1 Torr and 20 keV. In addition, the effect of Al₂O₃ content on the phase composition of fired pellets was discussed based on the thermodynamic calculations obtained using FactSage software (Version 8.0). Image-Pro Plus 6.0 was employed to analyze and calculate the perimeter and area of particles in the pellet.

The consolidation index (CI), particle growth index (GI), and particle uniformity index (UI) were further proposed to reveal the effect of aluminum occurrence on the consolidation behaviors of oxidized pellets in quantitative form [24]. The related computational formulas are expressed as Eqs. (1)–(3), respectively:

$$CI = (SPP - SPP') / SPP \quad (1)$$

$$GI = (APA - APA') / APA \quad (2)$$

$$UI = 1 - \sum_{i=1}^N |A_i - \bar{A}| / (N\bar{A}) \quad (3)$$

where CI refers to the perimeter change rate between oxidized and roasted pellets (roasting at 800°C for 30 min); SPP (SPP') is the sum of the perimeter of particles in the oxidized (roasting) pellets (μm); GI indicates the area change rate between oxidized and roasted pellets; APA (APA') represents the average area of particles in the oxidized (roasting) pellets (μm²); UI stands for the uniformity degree of particle size in an area; *N* is the total number of particles; *A_i* corresponds to the area of *i*-th particles (μm²); \bar{A} means the average area of particles in pellets (μm²).

3. Results and discussion

3.1. Thermodynamic properties of different aluminum types

To disclose the thermal behavior and phase transformation of different aluminum types at the constantly elevated

temperature of the oxidizing roasting process, the respective TG–DTG–DSC curves of gibbsite, hercynite, and kaolinite were analyzed, and the results are illustrated in Fig. 3. Fig. 3(a) shows that the weight loss process of gibbsite was completed at nearly 600°C with a weight loss ratio of 32.60%. Therein, the main dehydroxylation of the gibbsite started at around 200°C and gradually formed diaspores (AlOOH), as computed using Eq. (4). The first endothermic peak was observed at the elevated temperature of 298°C. The second endothermic peak was recorded at 523°C, and it was mainly attributed to the dehydroxylation of diaspores to form alumina (Al₂O₃), as shown by Eq. (5), with a weight loss ratio of 4.74%. For hercynite (Fig. 3(b)), a continuous mass gain can be observed because of the oxidation reaction (Eq. (6)) that transformed FeO to Fe₂O₃, with a weight gain rate of 2.91% as the temperature increased to 1250°C. By contrast, for kaolinite, its first endothermic peak occurred at 514°C because of the removal of its crystallization water, as proven by Eq. (7) (Fig. 3(c)). With the continued in the temperature, an exo-

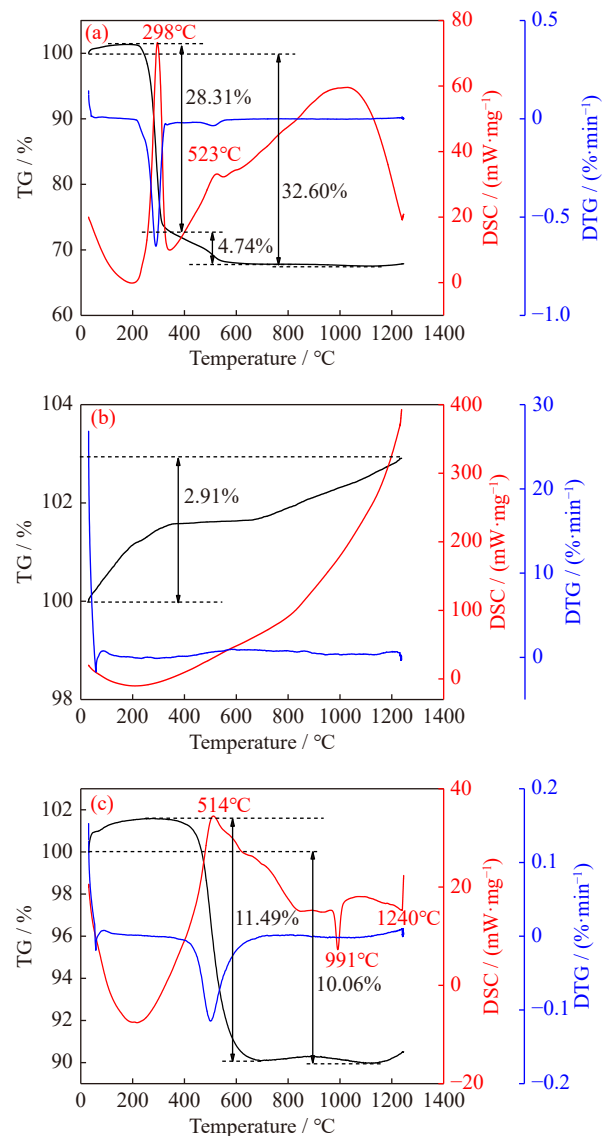
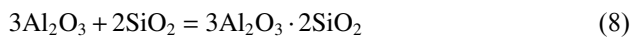
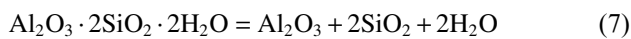
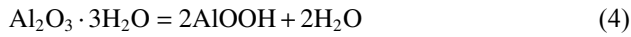


Fig. 3. TG–DTG–DSC curves of different aluminum types: (a) gibbsite; (b) hercynite; (c) kaolinite.

thermic peak appeared at 991°C due to the crystal transition of Al_2O_3 ($\alpha\text{-Al}_2\text{O}_3 \rightarrow \gamma\text{-Al}_2\text{O}_3$). However, the second exothermic peak at 1240°C was mainly caused by the combination reaction between Al_2O_3 and SiO_2 to form mullite ($\text{Al}_2\text{O}_3 \cdot 2\text{SiO}_2$), according to Eq. (8). Fig. 3(c) reveals a total weight loss of 10.06% from the TG curve. From the above results, the differences in the thermal behaviors of different aluminum types predictably affected the properties of preheated and fired pellets.



3.2. Effect of aluminum occurrence and content on the consolidation characteristics of pellets

3.2.1. Induration characteristics of preheated pellets

Fig. 4 shows the effect of aluminum occurrence and content on the CCS of preheated H and M pellets. For the H pel-

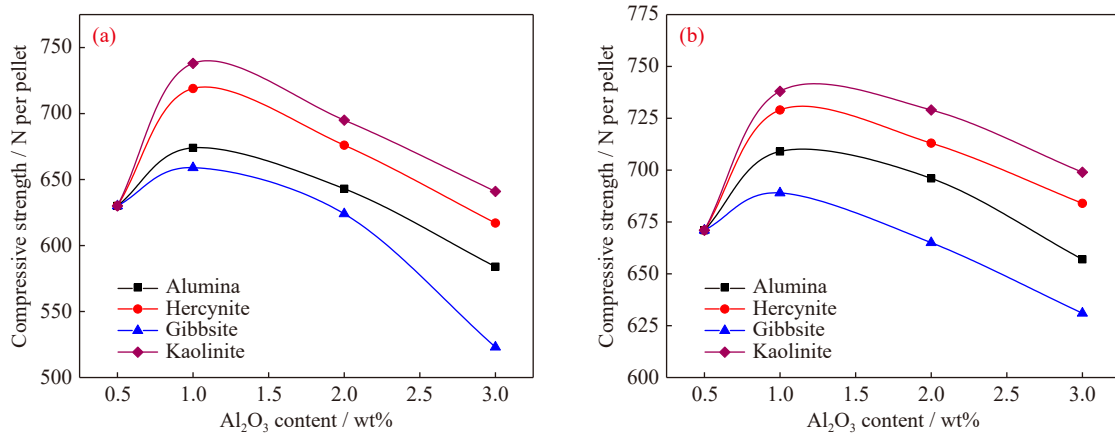


Fig. 4. Effect of aluminum occurrence and content on the CCS of preheated H (a) and M (b) pellets.

To a certain extent, finely-grained Al-containing additives can be used to optimize the size distribution of pellet feeds and increase the contact area of iron ore particles. As a result, the solid-phase reaction condition and connection bridges between ore particles improved during the preheating process. Hence, the alumina content remained at a low level of nearly 1.0wt%, which contributed to the increased CCS of the preheated pellets. However, the increased Al_2O_3 content deviated from the microcrystalline bonding observed between Fe_2O_3 particles because of the lower chemical activity of Al_2O_3 than hematite. Hercynite can transform into Fe_2O_3 and Al_2O_3 after an oxidation reaction. The newly generated Fe_2O_3 benefited the formation of microcrystalline bonding and relieved the adverse effect of excess Al_2O_3 content on the CCS of preheated pellets. Meanwhile, gibbsite and kaolinite had high LOI of 33.37wt% and 11.15wt%, respectively. The high LOI of the added Al-containing additives led to a high mass loss and large internal stress during

lets, when the Al_2O_3 content increased from the natural content to 1.0wt%, the corresponding CCS of the preheated pellets increased from 630 to 738, 719, 674, and 659 N per pellet with the addition of kaolinite, hercynite, free alumina, and gibbsite, respectively. As the Al_2O_3 content increased continuously from 1.0wt% to 3.0wt%, the CCS of preheated pellets with different aluminum types exhibited various downward trend levels. The adverse effects on CCS of the preheated H pellets from free alumina and gibbsite were more evident than those of preheated pellets from kaolinite and hercynite, respectively. Especially when the Al_2O_3 content in the preheated pellets reached 3.0wt% in the form of free alumina and gibbsite, the CCS were 584 and 523 N per pellet, respectively, which were notably lower than the value observed at natural Al_2O_3 content. For M pellets, with the increase in the Al_2O_3 content from natural content to 3.0wt%, the corresponding CCS of preheated pellets increased at first and then decreased with the addition of kaolinite, hercynite, free alumina, and gibbsite, which indicates a similar tendency to that of H pellets. However, compared with observation on M pellets, the increased Al_2O_3 content caused a more evidently unfavorable effect on the CCS of H pellets.

the preheating process, resulting in an adverse effect on the consolidation of preheated pellets. On the other hand, kaolinite, as a typical clay mineral, also acted as a binder and improved the ballability of iron ore concentrates and formed a denser structure for the green ball, which was beneficial to increase the CCS of the preheated pellet. Hence, the adverse effect degree of kaolinite on the consolidation of pellets was less than that observed for gibbsite.

3.2.2. Induration characteristics of fired pellets

Fig. 5 shows the results of the investigation on the effect of aluminum occurrence and content on the CCS of fired pellets. The results indicate that for H pellets when the alumina content in the form of gibbsite increased from natural content to 3.0wt%, the CCS of fired pellets decreased from 3752 to 2487 N per pellet. As for kaolinite, hercynite, and free alumina, the CCS of fired pellets was slightly elevated when the alumina content increased to 1.0wt%, and it gradually decreased as the alumina content increased further to 3.0wt%.

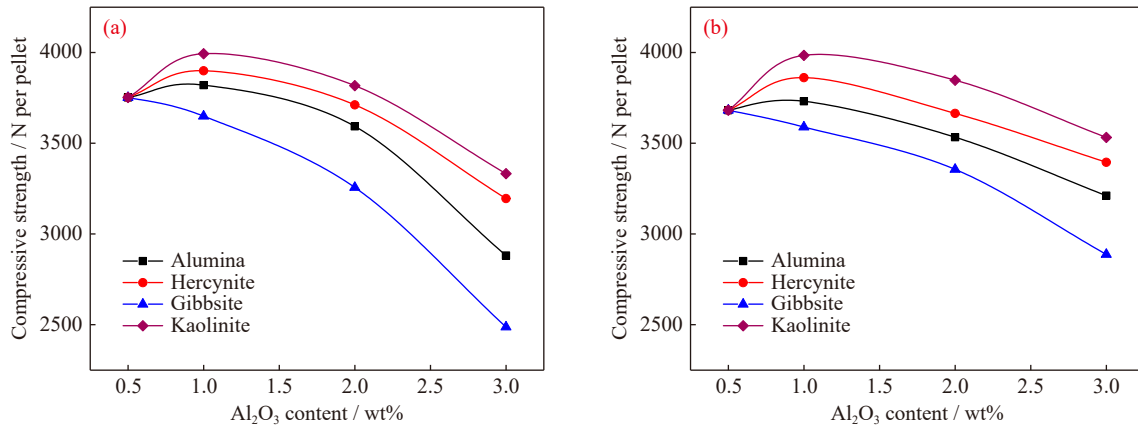


Fig. 5. Effect of types and content of aluminum on the compressive strength of fired H (a) and M (b) pellets.

At the same alumina content, kaolinite contributed to the relatively higher CCS of the fired pellets, followed by hercynite and free alumina. For the M pellets, as the alumina content of different alumina occurrences increased from natural content to 3.0wt%, the corresponding impact trend on the CCS of fired pellets was similar to that of H pellets. The effect extent of each alumina occurrence on the CCS of fired H pellets was more evident than that on the CCS of fired M pellets. This finding indicates that H pellets with a high-alumina content should be given more attention in terms of the CCS of fired pellets than M pellets.

In the case of fired pellets, recrystallization consolidation of Fe₂O₃ and liquid phase bonding benefited the preferable CCS. A certain amount of the liquid phase can accelerate the recrystallization and crystal growth of Fe₂O₃ and improve the consolidation and CCS of the fired pellets [11]. However, the increase in the Al₂O₃ content, to a certain extent, greatly increased the viscosity and limited the mass transfer effects of the reaction system because of its high melting point and low reactivity, adversely affecting the consolidation of fired pellets. Fig. 6 presents the quaternary phase diagram of SiO₂-CaO-Al₂O₃-MgO depending on the chemical compos-

ition of the fired pellets. With the increase of the Al₂O₃ from natural content to 3.0wt% (corresponding to point 0 to point 3) in the fired H (a) and M (b) pellets, the tendency of melting point for the slag decreased first and then increased. For the H pellets, the slag with the Al₂O₃ content of approximately 1.0wt% (point a₁) resulted in a low liquidus temperature below 1250°C, which can improve the liquid phase bonding among Fe₂O₃ particles.

For the different aluminum types, the oxidation of hercynite can generate Fe₂O₃ and Al₂O₃ accompanied by heat release, which benefits the recrystallization consolidation of Fe₂O₃. The excessive increase in the generated Al₂O₃ negatively affected the consolidation of the fired pellets. For gibbsite and kaolinite, the removal of crystal water at elevated temperatures resulted in micropores and fine cracks inside the fired pellets, which reduced the CCS. However, the adverse effect on fired pellets with kaolinite weakened because the suitable increase in SiO₂ generated from the thermal decomposition of kaolinite accelerated the formation of liquid phases, which improved the consolidation of the fired pellets.

3.3. Effect of aluminum occurrence on the consolidation behavior of pellets

3.3.1. Consolidation behavior of preheated pellets with different aluminum types

To further reveal the effect mechanism of aluminum types on the consolidation of preheated pellets, the microstructure and elemental distribution of preheated H and M pellets with different aluminum types were investigated, and the results are illustrated in Fig. 7 and Table 6. The particles underwent solid-phase diffusion, especially Fe₂O₃, and formed connection bridges with each other, which was the main contribution to the CCS of preheated pellets [4]. As shown in Fig. 7(a) and (b), compared with the preheated H pellets, the preheated M pellets with the same Al₂O₃ occurrence and content exhibited a preferable consolidation performance because the phase transformation from magnetite to hematite is an exothermic reaction, which can accelerate their solid-phase reaction with each other. Furthermore, for one type of iron ore, the pore morphology of the preheated pellets varied at the same alumina content for a different alumina occurrence. This condition indicates the variation in the effect de-

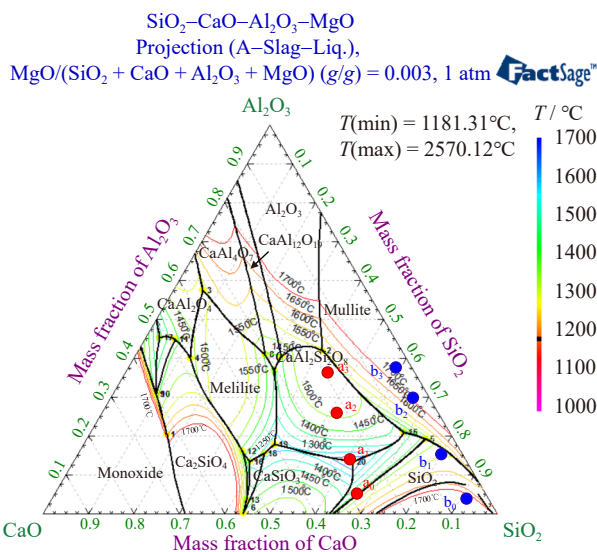


Fig. 6. Quaternary phase diagram of SiO₂-CaO-Al₂O₃-MgO (FactSage 8.0; points 0-3: natural, 1.0wt%, 2.0wt%, and 3.0wt% Al₂O₃ contents in the fired H (a) and M (b) pellets).

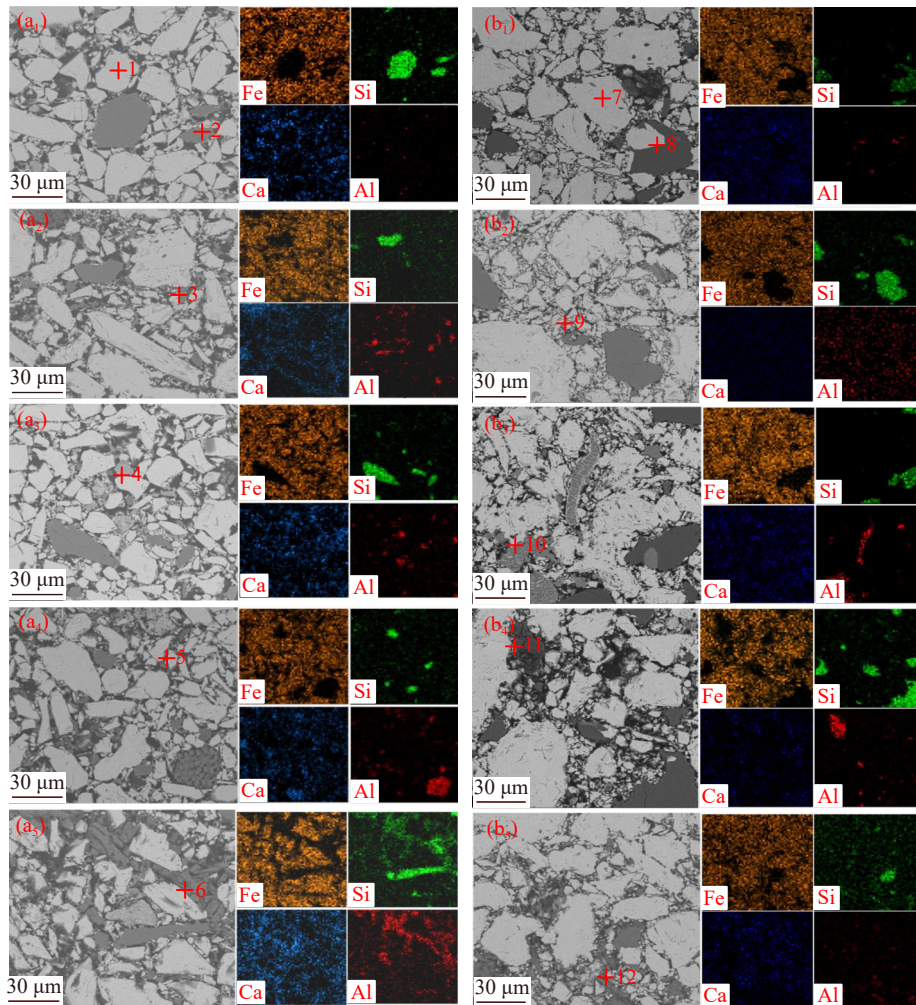


Fig. 7. Microstructure and elemental distribution of preheated H (a) and M (b) pellets with different Al-containing additives: (a1, b1) without Al-containing additive (natural Al_2O_3 content); with the addition of (a2, b2) alumina, (a3, b3) hercynite, (a4, b4) gibbsite, and (a5, b5) kaolinite, respectively, for 2.0wt% Al_2O_3 content.

Table 6. EDS analysis results for the spots in preheated pellets in Fig. 7

Spot	Elemental composition / wt%						Mineral phase
	Fe	Al	Si	Ca	Mg	O	
1	70.62	0.08	0.20	0.13	0.11	28.86	Hematite
2	1.03	—	43.34	—	—	55.63	Quartz
3	2.18	50.12	0.13	0.10	0.02	47.45	Alumina
4	38.37	24.31	0.34	0.25	0.08	36.65	Iron-aluminum oxides
5	3.52	48.13	1.14	0.89	0.03	46.29	Alumina
6	4.71	23.32	21.19	1.49	0.20	49.09	Anorthite
7	70.89	0.11	0.18	0.16	0.09	28.57	Hematite
8	2.11	—	42.37	—	—	55.52	Quartz
9	3.41	48.13	1.10	0.36	0.10	46.90	Alumina
10	35.98	23.87	2.19	1.10	0.89	35.97	Iron-aluminum oxides
11	4.31	48.89	1.10	0.33	0.81	44.56	Alumina
12	5.11	22.98	23.28	0.24	0.09	48.30	Anorthite

gree of each alumina occurrence on the consolidation of preheated pellets.

Compared with that of preheated pellets with natural alumina content (Fig. 7(a1) and (b1)), the size distribution of preheated pellets with separate addition of Al-containing additives (Fig. 7(a2–a5) and (b2–b5)) improved evidently via

fine-graded filling among the gaps of hematite particles. The compact distribution of particles was beneficial to the increase in the CCS of preheated pellets. The free alumina in preheated pellets mainly presented as an independent phase, which showed an unobvious consolidation with hematite particles because of its poor chemical reactivity. However,

the external diffusion of Fe from hematite to free alumina was attributed to their solid-phase reaction with each other, as proven by spots 3, 5, 9, and 11 in Fig. 7. This condition was conducive to the bonding of solid phases. For the preheated pellets with hercynite, the FeO in hercynite was oxidized to Fe₂O₃ (Fig. 7(a3) and (b3)). The phase transformation with a change in lattice accelerated the migration capacity of ions on the crystal surface, which benefited the crystal bonding between neighboring particles [22]. In addition, the exothermic oxidation of hercynite was a favorable factor for the consolidation of preheated pellets. However, the dense structure of hercynite resulted in limited reactivity for the further improvement of consolidation efficiency. For the preheated pellets with separate additions of gibbsite and kaolinite, more micropores and fine cracks can be observed, especially in the former (Fig. 7(a4–a5) and (b4–b5)). This finding deviates from the respective microcrystalline bonding and recrystallization between Fe₂O₃ particles.

Furthermore, from the map scanning of pellets with different aluminum types, the elements, such as Fe, Al, Si, and Ca, showed a certain degree of migration during the preheating process. The migration behavior was commonly attributed to the relatively low Tammann temperature and the crystal transfer and phase transformation during the preheating process. Therein, the Al in preheated pellets with kaolinite and gibbsite presented a more evident migration property than those with hercynite and free alumina. However, most of them were maintained in the Al-containing additives on site. Moreover, with the addition of CaCO₃ to improve the consolidation property of pellets, CaO was generated by the pyrolysis of CaCO₃. Ca²⁺ was mainly distributed around the particles of hematite, Al-containing phases, and quartz, which possibly contributed to their solid-phase reaction with each other during the preheating process, as proven by the migration of Ca (Fig. 7). After the thermal decomposition, the Si⁴⁺ from kaolinite exhibited a better reactivity for the solid-phase reaction than that from quartz. The generation of calcium ferro aluminosilicate (Fig. 7(a5) and (b5)) substantiated the migrations of Ca²⁺ and Fe³⁺. In sum, the differences in aluminum types resulted in evident effects on the consolidation efficiency of preheated pellets. In general, kaolinite was more beneficial to obtaining comparatively better consolidation performance of preheated pellets, followed by hercynite, free alumina, and gibbsite, consistent with the findings shown in Fig. 4.

3.3.2. Consolidation behavior of fired pellets from different aluminum types

Fig. 8 shows the microstructure and elemental distribution of fired H and M pellets with different Al-containing additives, and the related EDS analysis of mineral phases is illustrated in Table 7. The bonding degree between the particles in the pellets showed a remarkable improvement in the form of line–surface connection via a roasting process in comparison with the point connection observed in the preheating process. The high consolidation degree contributed to the great growth of crystal particles and the low porosity of

pellets. The preferable consolidation resulted in a desirable CCS for the fired pellets.

As displayed in Fig. 8(a) and (b), the fired M pellets with the same alumina content and occurrence showed a better consolidation performance in comparison with the fired H pellets because the newly generated hematite from the oxidation of magnetite caused the recrystallization of Fe₂O₃ in comparison with the original hematite. In general, in addition to the recrystallization of Fe₂O₃, the liquid phase bonding was an important consolidation form of the fired pellets. For the pellets with the addition of CaO, the calcium ferrite (CaO·Fe₂O₃) generated with a suitable content was suggested because of its better bonding strength and wettability than other liquid phases [5]. Hence, the calcium ferrite is commonly used to fill the gaps between solid particles and further accelerated the recrystallization of Fe₂O₃.

Furthermore, the microstructure of fired pellets with different aluminum occurrences (Fig. 8(a2–a5) and (b2–b5)) revealed that the recrystallization degree of Fe₂O₃ weakened to some extent in comparison with that with natural aluminum content. Thus, Al₂O₃ has a negative effect on the recrystallization of Fe₂O₃. As shown by the elemental distribution of fired pellets in Fig. 8(a2–a5) and (b2–b5), Al³⁺ showed a more evident elemental migration than that in the preheated pellets, and a large proportion of Al³⁺ remained enriched in the Al-containing additives on site. To further quantitatively evaluate the consolidation characteristics of oxidized pellets with different Al-containing additives, the effect of aluminum occurrence on the consolidation behaviors of oxidized pellets was observed (Fig. 9).

The results demonstrated that the different aluminum occurrences had a notable influence on the CI, GI, UI, and porosity of oxidized H and M pellets. As shown in Fig. 9(a), when the aluminum content of oxidized H pellets was increased to 2.0wt% with the separate addition of alumina, hercynite, gibbsite, and kaolinite, the CI varied from 0.43 to 0.37, 0.39, 0.30, and 0.46, respectively. The presence of Al₂O₃ caused difficulty in the particle interface removal. Fig. 9(b) shows the particle GI of H pellets with various Al-containing additives. Similar to the changes in CI, with the addition of different Al-containing additives, the GI of the particles varied from 1.73 to 1.48, 1.54, 1.35, and 1.60, which indicates that Al₂O₃ may restrict the formation of hematite crystals. Fig. 9(c) depicts the UI of particle dispersion in H pellets with various Al-containing additives. The figure reveals that when the Al₂O₃ content in the pellets increased from natural content to 2.0wt% via the addition of different Al-containing additives, the UI increased from 1.07 to 1.23, 1.18, 1.42, and 1.12. This result was mostly due to the differences in minerals and their low reactivity with each other, which impeded the formation of aluminum minerals and resulted in an uneven distribution of particles. Fig. 9(d) shows the porosity of H pellets with various Al-containing additives. The figure illustrates that when the Al₂O₃ content in the pellets increased from natural content to 2.0wt% with the separate addition of alumina, hercynite, gibbsite, and kaolin-

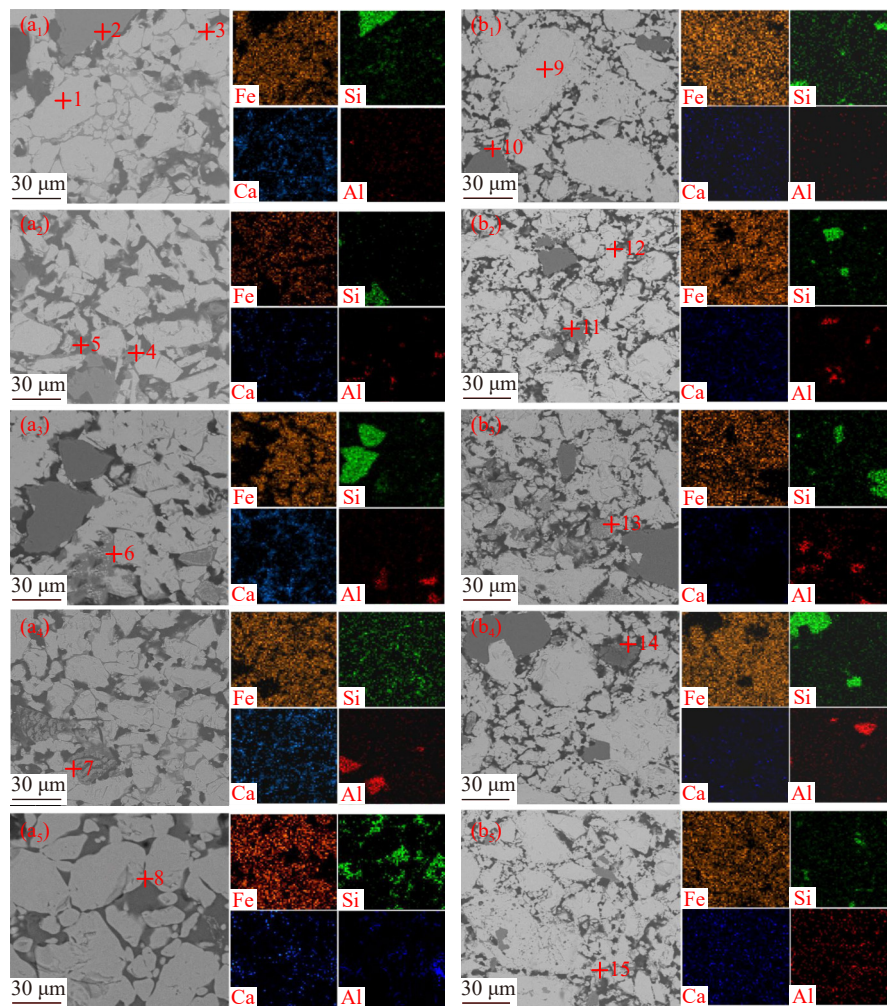


Fig. 8. Microstructure and elemental distribution of fired H (a) and M (b) pellets with different Al-containing additives: (a1, b1) without Al-containing additive (natural Al_2O_3 content); with the addition of (a2, b2) alumina, (a3, b3) hercynite, (a4, b4) gibbsite, and (a5, b5) kaolinite, respectively, for 2.0wt% Al_2O_3 content.

Table 7. EDS analysis results for the spots in the fired pellets in Fig. 8

Spot	Elemental composition / wt%						Mineral phase
	Fe	Al	Si	Ca	Mg	O	
1	69.39	0.24	0.41	0.25	0.20	29.51	Hematite
2	1.42	0.09	42.42	0.11	0.04	55.92	Quartz
3	44.23	0.19	4.91	12.31	0.20	38.16	Calcium ferrite
4	10.85	27.31	8.89	3.37	0.18	49.40	Calcium ferro aluminosilicate
5	3.19	46.74	1.99	0.31	0.09	47.68	Alumina
6	29.37	15.75	7.31	3.10	0.09	44.38	Calcium ferro aluminosilicate
7	12.98	29.45	10.31	3.81	0.11	43.34	Calcium ferro aluminosilicate
8	3.82	11.34	24.35	4.11	0.13	58.25	Calcium aluminosilicate
9	69.87	0.12	0.31	0.19	0.09	29.42	Hematite
10	1.98	0.03	42.89	0.10	0.02	54.98	Quartz
11	9.38	25.23	8.10	3.01	0.04	54.24	Calcium ferro aluminosilicate
12	2.21	45.87	1.82	0.28	0.04	49.78	Alumina
13	28.11	15.10	6.24	2.89	0.04	47.62	Calcium ferro aluminosilicate
14	10.81	27.71	8.36	3.07	0.09	49.96	Calcium ferro aluminosilicate
15	9.01	10.49	23.51	4.97	0.10	51.92	Calcium ferro aluminosilicate

ite, the porosity of H pellets varied from 15.2% to 18.1%, 17.4%, 21.8%, and 14.4%, respectively. The increase in the aluminum content had a detrimental effect on the shrinkage

of oxidized pellets. Furthermore, compared with M pellets, the H pellets showed lower CI and higher UI and porosity under the same aluminum occurrence and content condition.

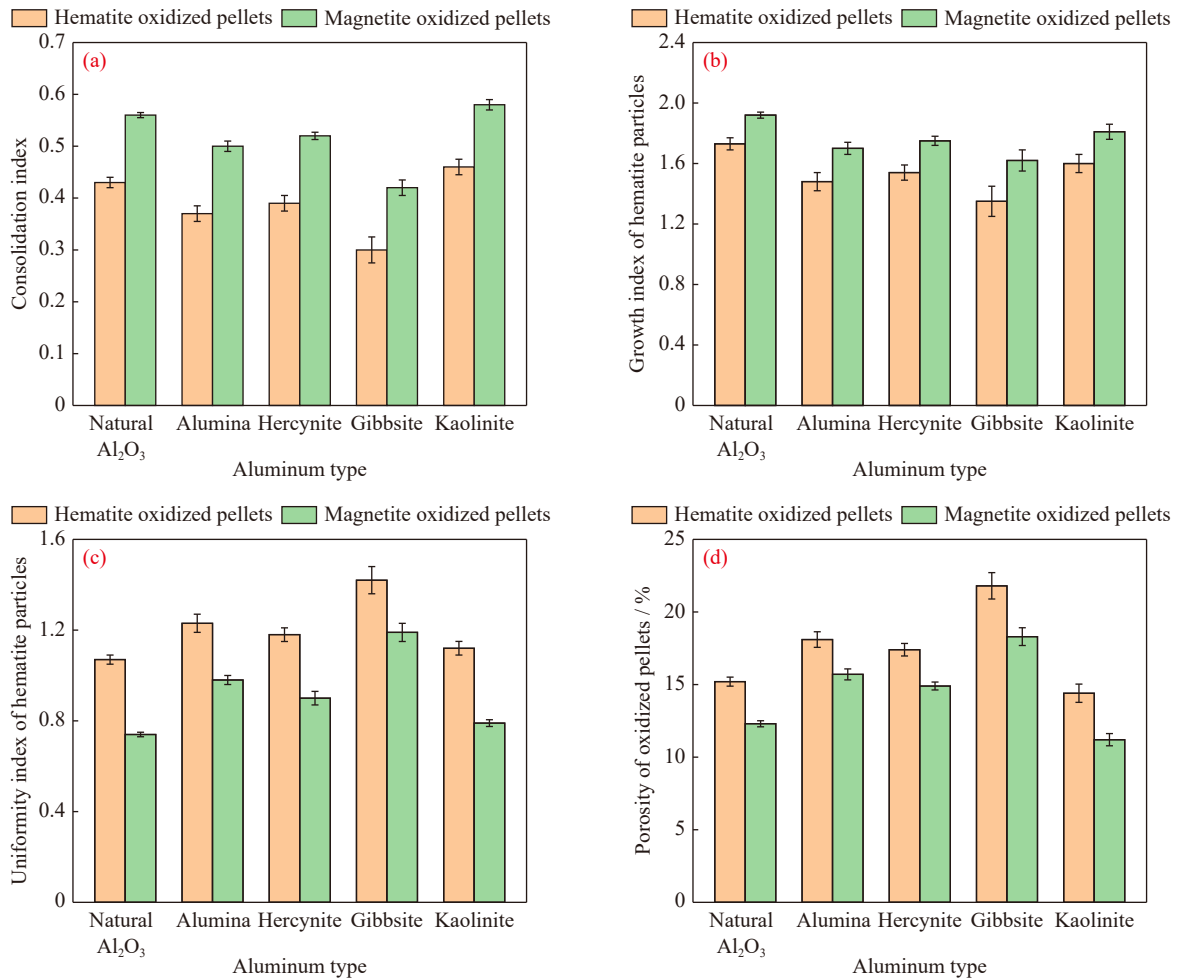


Fig. 9. Effect of aluminum occurrence on the consolidation behaviors of oxidized H and M pellets at natural Al_2O_3 content and with 2wt% Al_2O_3 by separate addition of alumina, hercynite, gibbsite, and kaolinite: (a) CI; (b) GI of hematite particles; (c) UI of H particles; (d) porosity of oxidized pellets.

The combined results in Figs. 7–9 indicate that compared with the bonding efficiency between the Fe_2O_3 particles, the Al-containing particles showed a poorer consolidation property with Fe_2O_3 particles. Hence, the excessive increase in aluminum content caused a decrease in the CCS of fired pellets. In addition, for the fired pellets with different aluminum types, the internal layer of hercynite particles maintained a dense structure. On the contrary, the external surface of the particles exhibited an evident solid-phase reaction. The consolidation performance may be attributed to the formation of a quaternary eutectoid of $CaO-Fe_2O_3-Al_2O_3-SiO_2$ between the particles of hercynite and hematite. The existence of quaternary eutectoid benefited the relatively high activity of Fe_2O_3 and Al_2O_3 generated by the oxidation reaction of hercynite. In addition, the quaternary eutectoid in the fired pellets with other aluminum occurrences improved the consolidation efficiency. However, in the fired pellets with gibbsite, the micropores and cracks generated from the thermal decomposition of gibbsite during the preheating stage still existed, which resulted in a remarkable decrease in the CCS of fired pellets. For the fired pellets with kaolinite, the adverse effect of crystal water removal of kaolinite on the CCS of pellets was substantially weakened by the formation of quaternary eutectoid filling the mineral particles, which enhan-

ced the consolidation performance. The newly generated SiO_2 and Al_2O_3 from the decomposition of kaolinite also contributed to the mass transfer effect and solid-phase reaction, as proven by the disappearance of the original shape of kaolinite.

3.3.3. Migration regularity of elements near the particle boundary of Al-containing phases in fired pellets

The high-heat solid-phase reactions of mineral particles in the pellets were commonly accompanied by mass transfer and element migration, and this condition affected the consolidation efficiency and CCS of the fired pellets [8]. Hence, the migration regularity of elements near the particle boundary of Al-containing phases in fired H pellets was further studied. Fig. 10(a) shows the energy spectrum and line scanning analysis of the reaction interface between hematite and quartz in the fired pellets at the natural aluminum content. Fe^{3+} exhibited a more evident diffusion behavior from hematite to quartz in comparison with Si^{4+} from quartz to hematite. At zone 3 (Fig. 10(a)) near the particle boundary, in addition to the 18.63wt% Fe^{3+} , 11.39wt% Ca^{2+} was detected, and this result was attributed to the diffusion behavior of Ca^{2+} . The migration of multiple elements benefited the formation of connection bridges between the particles of hematite and gangue minerals, which resulted in a preferable consolidation performance of the fired pellets.

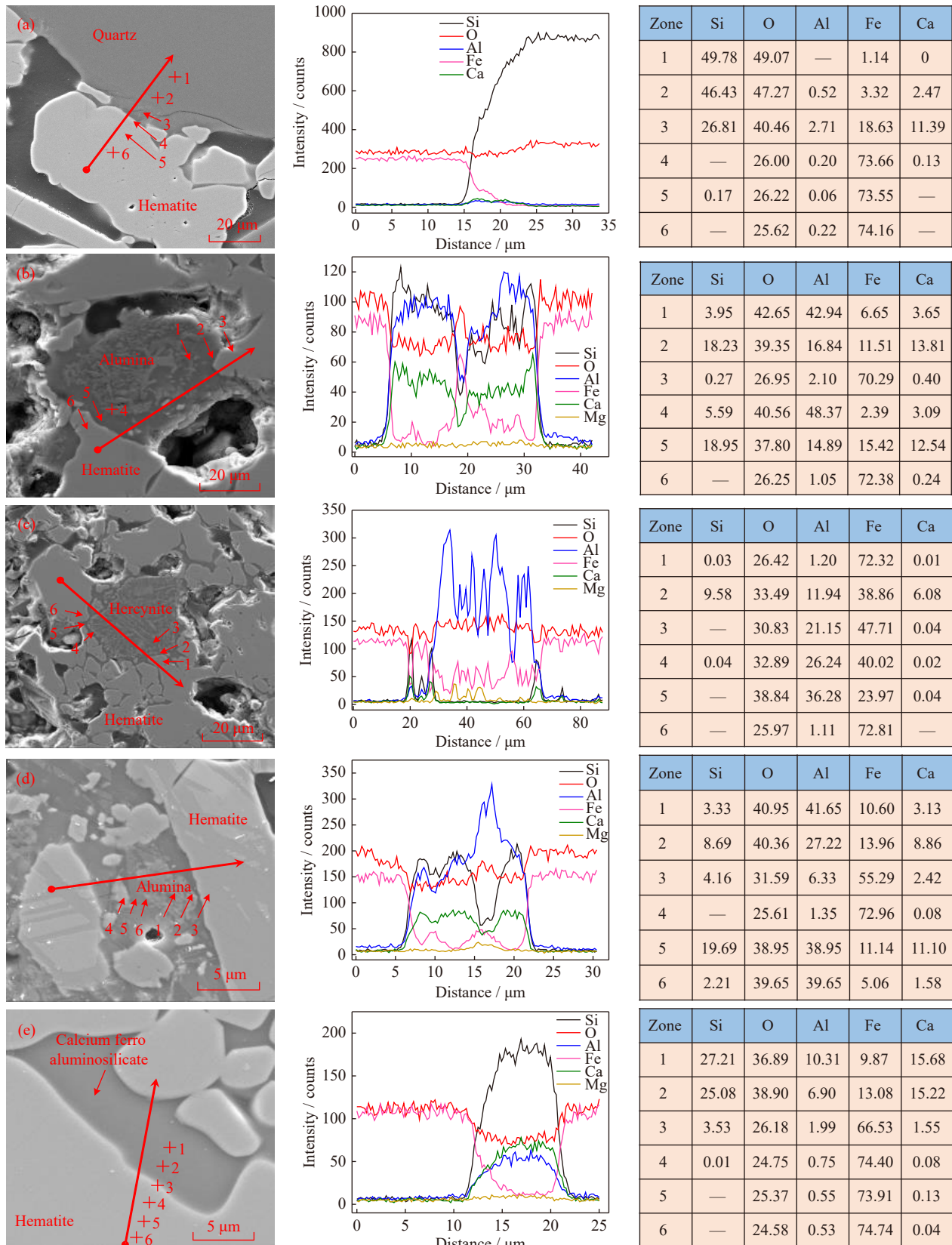


Fig. 10. Energy spectrum and line scanning analysis of the reaction interface near the particle boundary of Al-containing phases in the fired H pellets with (a) natural aluminum content, (b) alumina, (c) hercynite, (d) gibbsite, and (e) kaolinite.

Furthermore, with the addition of different Al-containing additives, the related migration regularity of elements was investigated to further reveal the effect mechanism of aluminum occurrence on the consolidation of pellets. Fig. 10(b)–(e)

illustrates the energy spectrum and line scanning analysis of the reaction interface near the particle boundary of Al-containing phases in the fired pellets with separated addition of free alumina, hercynite, gibbsite, and kaolinite.

As shown in Fig. 10(b), the Al content of 2.10wt% (zone 3) and Fe content of 6.65wt% (zone 1) can be detected in the interior phases of hematite and free alumina, respectively. Fe^{3+} had a more remarkable diffusion tendency from hematite to free alumina in comparison with that of Al^{3+} from free alumina to hematite. Zone 2 (Fig. 10(b)), which was located at the particle boundary between hematite and free alumina, was a transition region of elemental migration. In the transition region, aside from Fe^{3+} and Al^{3+} , Ca^{2+} and Si^{4+} can be detected. The existence of multiple elements benefited the formation of low-melting-point phases and their transformation into liquid phases during the roasting process, which enhanced the mass transfer. Combined with the line scanning results for the different phases, the diffusion of elements into the transition region from the free alumina and hematite particles was the main form that caused the adverse effect of low-activity free alumina particles on the consolidation efficiency. However, the formation of low-intensity aggregation and the existence of pores in large numbers deviated from the consolidation efficiency of pellets. Hence, the high content or excessive concentration of alumina resulted in the low CCS of fired pellets.

Fig. 10(c) illustrates that hercynite showed a more evident solid-phase reaction with other mineral particles at the roasting stage in comparison with that in the preheating stage due to the elevated temperature. The newly generated Fe_2O_3 and Al_2O_3 had a relatively good reactivity, which was beneficial to the migration of Fe and Al to the boundary of particles and the formation of a eutectoid with SiO_2 and CaO. The polybasic $\text{CaO-Fe}_2\text{O}_3\text{-Al}_2\text{O}_3\text{-SiO}_2$ eutectoid is a preferable slag layer on the exterior of hercynite particles, and it serves as a connection bridge to bond with the hematite particles. The formation of polybasic eutectoid is conducive to improving the consolidation efficiency of pellets. Furthermore, the complete oxidation of hercynite resulted in the composition segregation of Fe_2O_3 from FeO, which indicates the opposite distribution regularity of Al^{3+} and Fe^{3+} , as proven by the line scanning results in Fig. 10(c). However, the interior of hercynite particles still maintained a compact structure, which led to a less adverse effect on the CCS of fired pellets.

Furthermore, for the fired pellets with gibbsite, the fine cracks and pores of alumina particles, which were generated by the dehydroxylation of gibbsite during the preheating stage, still existed in the roasting stage and provided an advantageous condition for elemental migration. Hence, the interior of alumina particles can contain 8.29wt% Si^{4+} , 13.96wt% Fe^{3+} , and 8.86wt% Ca^{2+} in zone 2 (Fig. 9(d)). The line scanning results of alumina also revealed the strong spectral peaks of Si^{4+} , Fe, and Ca^{2+} . The multielement diffusion to alumina contributed to the formation of polybasic eutectic solutions. As a binding phase, the $\text{CaO-Fe}_2\text{O}_3\text{-Al}_2\text{O}_3\text{-SiO}_2$ eutectic solutions can fill in the interior of alumina particles to enhance the consolidation efficiency of Al-containing phases. However, limited by a large number of cracks and pores in the interior of the alumina particles, the beneficial effects of the adhesive property of polybasic eutectic solutions were insufficient to eliminate the adverse effect of the dehydroxylation of gibbsite. The generation of

cracks and pores caused an evident decrease in the consolidation efficiency and CCS of fired pellets.

For the fired pellets with kaolinite (Fig. 10(e)), the fine cracks and pores caused by the decomposition of kaolinite disappeared, and this result was attributed to the formation of polybasic eutectoid followed by the sufficient bonding of liquid phases. The sufferable porous structure inside the kaolinite particles provided a good diffusion condition for the newly generated Al_2O_3 and SiO_2 at the initial roasting stage, which benefited the generation of $\text{CaO-Fe}_2\text{O}_3\text{-Al}_2\text{O}_3\text{-SiO}_2$ via the combination with the Fe_2O_3 and CaO from hematite and calcium carbonate, respectively. The elemental migration also exhibited a regular gradient distribution, as revealed by the line scanning in Fig. 10(e), and no independent alumina particles were observed. Hence, the dense structure, which benefited from the addition of kaolinite to form a suitable bonding of liquid phases, was advantageous for the improvement of consolidation efficiency and CCS of fired pellets compared with other aluminum occurrences.

4. Conclusions

Based on their detection in typical iron ore concentrates, the effects of aluminum types, including alumina, hercynite, gibbsite, and kaolinite, on the consolidation efficiency of H and M pellets were determined by the addition of corresponding Al-containing additives, and the related mechanism was revealed. Conclusions were drawn as follows.

(1) During the preheating and roasting processes, the alumina from different aluminum sources adversely affected the induration characteristics of pellets, especially H pellets, because of its low chemical reactivity that impedes the recrystallization of Fe_2O_3 . Limited by the adverse effects, the suggested alumina content in pellets is below 2.0wt% or 1.0wt%, depending on the respective proportion of different aluminum types. In the fired pellets with the addition of CaO, aluminum was commonly present in the form of alumina, hercynite, calcium aluminosilicate, and calcium ferro aluminosilicate.

(2) The thermal decomposition of gibbsite and kaolinite generated internal stress and fine cracks, which deviated from the respective microcrystalline bonding and recrystallization between Fe_2O_3 particles. The adverse effects on the induration characteristics of fired pellets with different aluminum types can be relieved to varying degrees through the formation of slag bonds of polybasic $\text{CaO-Fe}_2\text{O}_3\text{-Al}_2\text{O}_3\text{-SiO}_2$ eutectic solution between the particles of aluminum-bearing compound and H in the presence of CaO. Kaolinite was more beneficial to the induration process than the other three aluminum minerals because of the formation of a more liquid phase, which improved the consolidation of the resultant pellets.

Acknowledgements

This work was financially supported by the National Natural Science Foundation of China (Nos. 52004339 and

52174329), the Fundamental Research Funds for the Central Universities, China (No. N2325031), and the China Baowu Low Carbon Metallurgy Innovation Foundation (No. BWL-CF202216). The authors would like to thank the Fundamental Research Funds for the Central Universities of Central South University, which supplied us with the facilities and funds to fulfill the experiments.

Conflict of Interest

Mansheng Chu is an editorial board member for IJMMM and is not involved in the editorial review or the decision to publish this article. The authors declare no potential conflict of interest.

References

- [1] C. Wang, C.Y. Xu, Z.J. Liu, Y.Z. Wang, R.R. Wang, and L.M. Ma, Effect of organic binders on the activation and properties of indurated magnetite pellets, *Int. J. Miner. Metall. Mater.*, 28(2021), No. 7, p. 1145.
- [2] D.Q. Zhu, W.Q. Huang, C.C. Yang, X. Hu, and J. Pan, Technical progress in iron ore pelletization, *Sintering and Pelletizing*, 42(2017), No. 3, p. 42.
- [3] T. Jiang, Y.B. Zhang, Z.C. Huang, G.H. Li, and X.H. Fan, Pre-heating and roasting characteristics of hematite-magnetite (H-M) concentrate pellets, *Ironmaking Steelmaking*, 35(2008), No. 1, p. 21.
- [4] F. Zhang, D.Q. Zhu, J. Pan, Z.Q. Guo, and M.J. Xu, Improving roasting performance and consolidation of pellets made of ultrafine and super-high-grade magnetite concentrates by modifying basicity, *J. Iron Steel Res. Int.*, 27(2020), No. 7, p. 770.
- [5] D.Q. Zhu, F. Zhang, Z.Q. Guo, J. Pan, and W. Yu, Grate-kiln pelletization of Indian hematite fines and its industrial practice, *Int. J. Miner. Metall. Mater.*, 24(2017), No. 5, p. 473.
- [6] A.B. Kotta, A. Patra, M. Kumar, and S.K. Karak, Effect of molasses binder on the physical and mechanical properties of iron ore pellets, *Int. J. Miner. Metall. Mater.*, 26(2019), No. 1, p. 41.
- [7] J.J. Dong, G. Wang, Y.G. Gong, Q.G. Xue, and J.S. Wang, Effect of high alumina iron ore of gibbsite type on sintering performance, *Ironmaking Steelmaking*, 42(2015), No. 1, p. 34.
- [8] G.H. Li, M.D. Liu, T. Jiang, T.H. Zhou, and X.H. Fan, Mineralogy characteristics and separation of aluminum and iron of high-aluminum iron ores, *J. Cent. South Univ. Sci. Technol.*, 40(2009), No. 5, p. 1165.
- [9] S.W. Kim, J.W. Jeon, I.K. Suh, and S.M. Jung, Improvement of sintering characteristics by selective granulation of high Al₂O₃ iron ores and ultrafine iron ores, *Ironmaking Steelmaking*, 43(2016), No. 7, p. 500.
- [10] H. Sahoo, S.S. Rath, D.S. Rao, B.K. Mishra, and B. Das, Role of silica and alumina content in the flotation of iron ores, *Int. J. Miner. Process.*, 148(2016), p. 83.
- [11] A.B. Kotta, D. Narsimhachary, S.K. Karak, and M. Kumar, Studies on the mechanical and physical properties of hematite iron ore pellets prepared under different conditions, *Trans. Indian Inst. Met.*, 73(2020), No. 10, p. 2561.
- [12] A. Ghosh, B. Nayak, T.K. Das, and S. Palit Sagar, A non-invasive technique for sorting of alumina-rich iron ores, *Miner. Eng.*, 45(2013), p. 55.
- [13] G.H. Li, T. Jiang, M.D. Liu, T.H. Zhou, X.H. Fan, and G.Z. Qiu, Beneficiation of high-aluminium-content hematite ore by soda ash roasting, *Miner. Process. Extr. Metall. Rev.*, 31(2010), No. 3, p. 150.
- [14] X.G. Hu, H.Y. Zheng, Y.C. Guo, X. Jiang, Q.J. Gao, and F.M. Shen, Determination of Al₂O₃ activity by reference slag method in CaO-SiO₂-Al₂O₃-MgO melts for blast furnace slag with high Al₂O₃ at 1873 K, *Steel Res. Int.*, 91(2020), No. 3, art. No. 1900285.
- [15] T. Murakami, S. Nakamura, D. Maruoka, and E. Kasai, Effects of iron ore type and gangue mineral components on strength of sintered fine powder granule, *Tetsu-to-Hagane*, 107(2021), No. 6, p. 463.
- [16] Y.F. Chai, W.T. Yu, J.L. Zhang, S.L. An, J. Peng, and Y.Z. Wang, Influencing mechanism of Al₂O₃ on sintered liquid phase of iron ore fines based on thermal and kinetic analysis, *Ironmaking Steelmaking*, 46(2019), No. 5, p. 424.
- [17] N.A.S. Webster, D.P. O'dea, B.G. Ellis, and M.I. Pownceby, Effects of gibbsite, kaolinite and Al-rich goethite as alumina sources on silico-ferrite of calcium and aluminium (SFCA) and SFCA-I iron ore sinter bonding phase formation, *ISIJ Int.*, 57(2017), No. 1, p. 41.
- [18] J.L. Zhang, Z.Y. Wang, X.D. Xing, and Z.J. Liu, Effect of aluminum oxide on the compressive strength of pellets, *Int. J. Miner. Metall. Mater.*, 21(2014), No. 4, p. 339.
- [19] F.M. Shen, Q.J. Gao, X. Jiang, G. Wei, and H.Y. Zheng, Effect of magnesia on the compressive strength of pellets, *Int. J. Miner. Metall. Mater.*, 21(2014), No. 5, p. 431.
- [20] X.B. Li, H.Y. Wang, Q.S. Zhou, *et al.*, Reaction behavior of kaolinite with ferric oxide during reduction roasting, *Trans. Non-ferrous Met. Soc. China*, 29(2019), No. 1, p. 186.
- [21] Y.H. Guo, J. Xie, J.J. Gao, H.J. Xu, and J.M. Qie, Study on the production and metallurgical properties of fluxed pellets with high hematite content, *Metallurgist*, 61(2017), No. 7-8, p. 638.
- [22] Y.X. Xue, J. Pan, D.Q. Zhu, *et al.*, Effect of alumina occurrence on sintering performance of iron ores and its action mechanism, *J. Mater. Res. Technol.*, 12(2021), p. 1157.
- [23] L. Lu, R.J. Holmes, and J.R. Manuel, Effects of alumina on sintering performance of hematite iron ores, *ISIJ Int.*, 47(2007), No. 3, p. 349.
- [24] Y.Z. Wang, J. Schenk, J.L. Zhang, *et al.*, Novel sintering indexes to evaluate and correlate the crystal characteristics and compressive strength in magnetite pellets, *Powder Technol.*, 362(2020), p. 517.